

# Effect of refractive index on the fluorescence lifetime of green fluorescent protein

Carolyn Tregidgo

James A. Levitt

Klaus Suhling

King's College London

Department of Physics

Strand

London, WC2R 2LS, United Kingdom

E-mail: klaus.suhling@kcl.ac.uk

**Abstract.** The average fluorescence lifetime of the green fluorescent protein (GFP) in solution is a function of the refractive index of its environment. We report that this is also the case for GFP-tagged proteins in cells. Using time-correlated single-photon counting (TCSPC)-based fluorescence lifetime imaging (FLIM) with a confocal scanning microscope, images of GFP-tagged proteins in cells suspended in different refractive index media are obtained. It is found that the average fluorescence lifetime of GFP decreases on addition of glycerol or sucrose to the media in which the fixed cells are suspended. The inverse GFP lifetime is proportional to the refractive index squared. This is the case for GFP-tagged major histocompatibility complex (MHC) proteins with the GFP located inside the cytoplasm, and also for GPI-anchored GFP that is located outside the cell membrane. The implications of these findings are discussed with regard to total internal reflection fluorescence (TIRF) techniques where the change in refractive index is crucial in producing an evanescent wave to excite fluorophores near a glass interface. Our findings show that the GFP fluorescence lifetime is shortened in TIRF microscopy in comparison to confocal microscopy. © 2008 Society of Photo-Optical Instrumentation Engineers. [DOI: 10.1117/1.2937212]

**Keywords:** fluorescence lifetime imaging (FLIM); refractive index; green fluorescent protein; total internal reflection fluorescence; time-correlated single-photon counting.

Paper 07337SSR received Aug. 17, 2007; revised manuscript received Dec. 19, 2007; accepted for publication Dec. 21, 2007; published online Jun. 20, 2008.

## 1 Introduction

Since the discovery that the green fluorescent protein (GFP) of the jellyfish *Aequorea victoria* can be genetically encoded in other organisms and still maintain its ability to fluoresce,<sup>1</sup> it has been widely used in the field of biophotonics with applications ranging from membrane trafficking to protein-protein interaction<sup>2</sup> and as such has made a huge impact on these areas. Breakthroughs in modern laser technology and confocal microscopy<sup>3</sup> have also greatly helped and facilitated many advances in the biological, biomedical, or, in general, life sciences.

In the last decade or so, fluorescence lifetime imaging (FLIM) has increasingly been used to image not only the location of particular proteins, but also their environment.<sup>4-8</sup> GFP in particular is routinely used as the donor in Förster resonance energy transfer (FRET) experiments,<sup>9-11</sup> and detecting FRET by FLIM is a good approach: It has the advantage of high signal-to-noise ratio and allows the distinction between FRET efficiency and FRET population.<sup>12,13</sup>

Due to the fact that GFP is so widely used, it is important to know what factors affect its fluorescence lifetime. In solution, the average GFP fluorescence lifetime was experimentally found to be inversely proportional to the square of its

refractive index,<sup>14,15</sup> in agreement with the theoretical prediction of the Strickler-Berg formula. This effect is also known to affect the fluorescence lifetime of organic dyes (and quantum dots<sup>16</sup>), and has been experimentally verified on various occasions.<sup>17-27</sup> It has, for example, been exploited to determine the refractive index of frozen gas matrices via the fluorescence lifetime of fluorophores embedded in them.<sup>28</sup>

Recently, it was also experimentally demonstrated that the refractive index of the medium affects the fluorescence lifetime of cyan fluorescent protein (CFP) and yellow fluorescent proteins (YFP) in solution.<sup>29</sup> In addition, fluorescence lifetime studies of GFP in reverse micelles show that the average fluorescence lifetime of GFP is shorter in the water pool of reverse micelles surrounded by isoctane (with a refractive index  $n=1.39$ ) or dodecane ( $n=1.42$ ) than in buffer alone.<sup>30</sup> However, few studies have been carried out to investigate whether the same is true for GFP-tagged proteins in cells. There is evidence that tagging GFP to a specific protein does not appear to affect the GFP fluorescence lifetime significantly.<sup>31,32</sup>

Here, we measure the average fluorescence lifetime of GFP-tagged proteins in cells as a function of the refractive index of the medium in which the cells are suspended. Moreover, in order to address the question over which distance the GFP fluorescence lifetime can sense the refractive index, we

Address all correspondence to Klaus Suhling, Physics King's College London Strand, London, UK WC2R 2LS United Kingdom; Tel: 020 7848 2119; Fax: 020 7848 2420; E-mail: klaus.suhling@kcl.ac.uk

employ time-resolved total internal reflection fluorescence (TIRF) microscopy. In TIRF microscopy, an evanescent wave is produced in a low refractive index medium by total internal reflection of an exciting beam in a high refractive index medium at an interface between the two.<sup>33,34</sup> The penetration depth of the evanescent wave is a function of the incident angle of the exciting beam, and is of the order of a few 100 nm or so. We carry out GFP fluorescence lifetime studies as a function of excitation angle in TIRF microscopy.

### 1.1 Fluorescence Lifetime as a Function of the Refractive Index

Fluorescence is the radiative deactivation of the lowest vibrational energy level of the first electronically excited singlet state of a fluorescent molecule. The fluorescence lifetime,  $\tau$ , is the average time a fluorophore remains in the excited state after excitation and is defined as the inverse of the sum of the rate parameters for all depopulation processes:

$$\tau = \frac{1}{k_r + k_{nr}}, \quad (1)$$

where  $k_r$  is the radiative rate constant, and the nonradiative rate constant,  $k_{nr}$ , is the sum of the rate constant for internal conversion,  $k_{ic}$ , and the rate constant for intersystem crossing to the triplet state,  $k_{isc}$ , so that  $k_{nr} = k_{ic} + k_{isc}$ .  $\tau_0$  is the natural or radiative lifetime, with  $\tau_0 = k_r^{-1}$ .

It has been known for some time that  $\tau_0$  is dependent on the refractive index, as reviewed in Ref. 35. For example, this is shown from the widely used Strickler-Berg formula, which relates absorption and emission spectra to the radiative lifetime<sup>36</sup>:

$$\frac{1}{\tau_0} = k_r = 2.88 \times 10^{-9} n^2 \frac{\int I(\nu) d\nu}{\int I(\nu) \nu^{-3} d\nu} \int \frac{\varepsilon(\nu)}{\nu} d\nu, \quad (2)$$

where  $n$  is the refractive index,  $I$  is the emission intensity,  $\varepsilon$  is the extinction coefficient, and  $\nu$  is the frequency of the transition in wavenumbers. A recent, more accurate treatment taking into account the transition dipole moment, an intrinsic property of the molecule, has been devised by Toptygin in an excellent review of the subject.<sup>35</sup>

Previous work carried out in our group has shown that by monitoring the variation in fluorescence lifetime of GFP across an interface of two different media, a change in refractive index can be sensed up to one micron from the interface.<sup>37,38</sup>

### 1.2 Fluorescence Lifetime at an Interface

Consider the equation of motion of the excited state dipole [Eq. (3)]. When the fluorescent molecule emits near an interface of two different refractive index media, there are partial reflections at the interface, resulting in interference of the reflected field and the excited state dipole. This reflected field damps the oscillating dipole, shortening the lifetime, and can be thought of much like stimulated emission.<sup>39</sup>

$$\ddot{\mu} + \omega^2 \mu = \frac{e^2}{m} E_R - b_0 \dot{\mu}. \quad (3)$$

$\mu$  is the dipole moment (the single and double dots indicate the first and second derivative with respect to time),  $E_R$  is the reflected field,  $b_0$  is the damping constant (the energy loss in radiation and in thermal, vibration processes, i.e., the inverse fluorescence lifetime,  $\tau^{-1}$ ),  $\omega$  is the oscillation frequency,  $e$  is the electronic charge, and  $m$  is its effective mass.

This equation can be solved to find the fluorescence lifetime as a function of distance from an interface. Tews<sup>40</sup> and Drexhage<sup>41</sup> found that parallel to the interface, the relative fluorescence lifetime,  $\tau_\infty / \tau_x^{para}$ , where  $\tau_x$  is the lifetime at a distance  $x$  from the interface, and  $\tau_\infty$  is the fluorescence lifetime in the absence of an interface, is given by:

$$\frac{\tau_\infty}{\tau_x^{para}} = 1 + \frac{3}{4} \phi \int_0^1 [R_s \cos(\delta_s + \gamma\Delta) - \gamma^2 R_p \cos(\delta_p + \gamma\Delta)] d\gamma, \quad (4)$$

while perpendicular to the interface  $\tau_\infty / \tau_x^{perp}$  is given by:

$$\frac{\tau_\infty}{\tau_x^{perp}} = 1 + \frac{3}{2} \phi \int_0^1 (1 - \gamma^2) R_p \cos(\delta_p + \gamma\Delta) d\gamma. \quad (5)$$

Assuming the emitting dipoles are randomly orientated, Eqs. (4) and (5) can be used to find the fluorescence lifetime of an isotropic distribution  $\tau_x^{is}$ :

$$\frac{1}{\tau_x^{is}} = \frac{2}{3\tau_x^{para}} + \frac{1}{3\tau_x^{perp}}. \quad (6)$$

$\phi$  is the quantum yield in the absence of the interface. The term  $\Delta$  is equal to  $4\pi x / \lambda$ , where  $\lambda$  is the emission wavelength of the fluorophore in its medium,  $\gamma = \cos \theta$ , where  $\theta$  is the angle of incidence of the emitted light on the interface,  $R_p$  and  $R_s$  are the Fresnel reflection coefficients parallel and perpendicular to the plane of incidence, respectively, and  $\delta_s$  and  $\delta_p$  are the phase shifts perpendicular and parallel, respectively.<sup>40</sup> Equation (6) thus tells us how the fluorescence lifetime should vary as a function of distance from a dielectric interface.

### 1.3 Total Internal Reflection Fluorescence (TIRF)

Total internal reflection fluorescence (TIRF) microscopy relies upon a change in refractive index at an interface to produce an evanescent wave that in turn can excite fluorescent molecules. The evanescent wave penetrates only a few 100 nm into the sample depending on the angle of incidence, making TIRF an excellent technique for probing thin sections and in particular cell/substrate contacts and single molecules fluorescing near a glass surface.<sup>34</sup>

When a beam of light travels from a high refractive index medium into a lower refractive index medium and the angle of incidence is greater than the critical angle,  $\theta_c$ , total internal reflection takes place. Upon solving Maxwell's equations, it is found that some light penetrates into the sample in the  $z$  direction (perpendicular to the interface), and this is known as the evanescent wave. The intensity of this evanescent wave decays exponentially in the form<sup>33,34</sup>

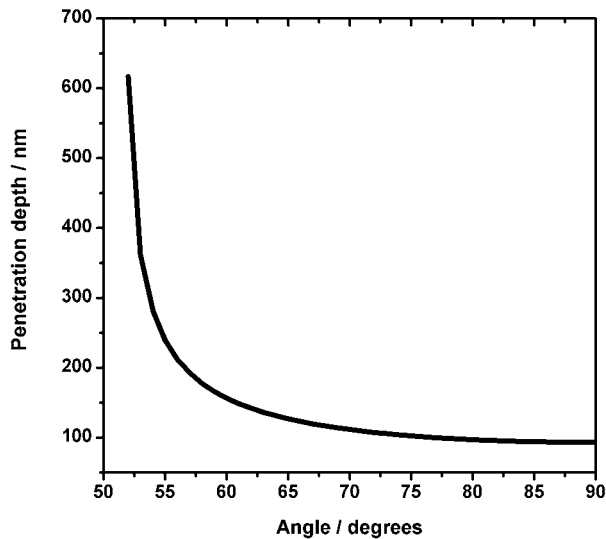


**Fig. 1** Evanescent wave penetration depth as a function of incident angle. This is calculated for an interface with a glass prism of refractive index  $n=1.70$  and a fluorescent sample in buffer solution ( $n=1.33$ ) according to Eqs. (7) and (8). The critical angle is  $51.5^\circ$ , and the excitation wavelength is  $467\text{ nm}$ .

$$I(z) = I(0)e^{-z/d}, \quad (7)$$

where  $I(z)$  is the intensity of the wave a distance  $z$  from the interface, i.e., perpendicular to the interface,  $I(0)$  is the intensity at the interface, and  $d$  is the penetration depth:

$$d = \frac{\lambda_0}{4\pi} (n_1^2 \sin^2 \theta - n_2^2)^{-1/2}, \quad (8)$$

where  $n_1$  is the refractive index of medium 1 (glass prism),  $n_2$  is the refractive index of medium 2 (liquid sample), and  $\lambda_0$  is the wavelength of the incident light in vacuum. For a double extra-dense flint glass prism ( $n_1=1.70$ ) exciting a sample in aqueous solution ( $n_2=1.33$ ), the penetration depth varies, as shown in Fig. 1. If the sample is excited at different angles of incidence, the distance the evanescent wave penetrates changes, and hence the distance from the interface at which the sample is excited also changes. Therefore, obtaining fluorescence decays or FLIM images at varying incident angles will allow the effect of TIRF coupled with time-resolved detection to be monitored.

## 2 Experimental Details

### 2.1 FLIM

The refractive index of the media, into which the cells were added, was varied by changing the concentrations of glycerol ( $\text{C}_3\text{H}_8\text{O}_3$ , molecular weight 92.09, Sigma Aldrich) in water. The cells, which were in PBS buffer, were then added to the glycerol solutions at a ratio of  $100\ \mu\text{l}$  glycerol solution to  $5\ \mu\text{l}$  cell solution. A further set of samples was made using different concentrations of sucrose in water to make sure that the observed effects were due only to the refractive index and not to the type of solution. The refractive index of the solutions was measured using a refractometer at  $589\text{ nm}$  before the addition of the cells. The cell lines investigated were cells

expressing class I major histocompatibility complex (MHC) protein tagged with GFP (HLA-CW6 GFP 721.221) and glycosylphosphatidylinositol (GPI)-anchored GFP (YTS/KIR2DL1-GPI-GFP).<sup>42</sup> The GFP mutant is enhanced GFP (EGFP), i.e., GFP F64L, S65T. The class I MHC is a transmembrane protein, and the GFP is attached to the intracellular C terminus of the MHC protein.<sup>43,44</sup> The GPI-anchored GFP is membrane-bound in the outer leaflet of the lipid bilayer, and the GFP is located outside the plasma membrane.<sup>45</sup> Thus, where the MHC protein is tagged, the GFP is located just inside the plasma membrane, whereas in the GPI-anchored GFP, it is located just on the outside of the membrane. Both cell lines were fixed using two different methods: The first was to fix using BD cytofix/cytoperm, and the second was to fix using 4% paraformaldehyde.

FLIM images of  $256 \times 256$  pixels were obtained using a Leica TCS SP2 inverted scanning confocal microscope coupled with a Becker & Hickl time-correlated single-photon counting (TCSPC) card SPC830 in a 3-GHz, Pentium IV, 1-GB RAM computer running Microsoft Windows XP. A Ti:Sapphire oscillator (Coherent Mira 900 with a center wavelength of  $900\text{ nm}$ , pulse duration  $\sim 180\text{ fs}$ , and repetition rate  $76\text{ MHz}$ ) pumped by a 6-W solid state-laser (Coherent Verdi V6) was used as the excitation source. Imaging was carried out with a  $63\times$  water immersion objective (numerical aperture  $\text{NA}=1.2$ ) and a line scanning speed of  $400\text{ Hz}$ . The emission was collected through a  $525 \pm 25\text{-nm}$  bandpass filter onto a cooled PMC 100-01 photomultiplier detector (Becker & Hickl, based on a Hamamatsu H5772P-01 photomultiplier). The acquisition time was  $500\text{ s}$  for each image. The average fluorescence lifetime of GFP was then found for each pixel in the image by fitting a single exponential using Becker & Hickl SPCImage software.

### 2.2 TIRF

The scanning confocal microscope used in Sec. 2.1 was adapted for TIRF by positioning a prism on top of the sample mount, with the sample between a coverslip and the prism. A sample of GFP in solution (EGFP, i.e., GFP F64L, S65T, courtesy of Dr. James Hunt, Randall Division of Cell and Molecular Biophysics at King's College, London) was then illuminated from above using a pulsed diode laser at  $467\text{ nm}$  (PLP-10 470, Hamamatsu) with a pulse duration of  $90\text{ ps}$  and a repetition rate of  $20\text{ MHz}$ . The emission from the EGFP in solution was collected in transmission through a  $10\times$  objective ( $\text{NA}=0.3$ ) (see Fig. 2). The angle of the incident laser beam could be varied from  $40^\circ$  to  $80^\circ$  so that below the critical angle ( $51.5^\circ$ ), there was bulk excitation, and at high angles, the evanescent wave penetration depth went down to  $\sim 100\text{ nm}$ , i.e., exciting only molecules within  $100\text{ nm}$  from the interface. Single fluorescence decays were detected using the Becker & Hickl SPC830 card described in Sec. 2.1 and were fitted to a single exponential to find the average fluorescence lifetime using Becker & Hickl SPCImage software.

## 3 Results and Discussion

### 3.1 FLIM Measurements

FLIM images of the cells expressing GFP-tagged MHC protein in phosphate buffered saline (PBS) buffer and in 100%

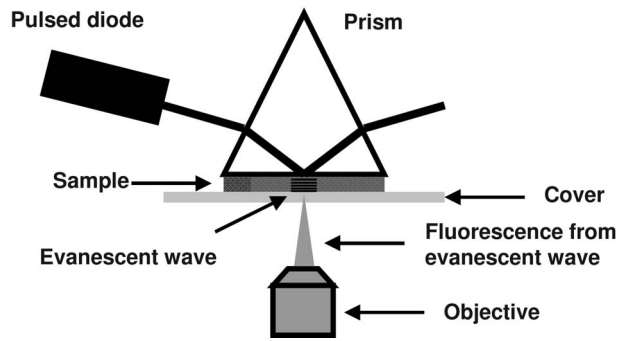


**Fig. 2** Experimental setup for TIRF with an inverted microscope. Excitation was from above using a pulsed diode laser, and fluorescence due to the evanescent wave was collected below through the microscope objective.

glycerol are shown in Fig. 3. GFP-tagged proteins in cells exhibit a shortening of the average GFP fluorescence lifetime as the proportion of the glycerol or sucrose in solution increases, as shown in Fig. 4. This can be seen more quantitatively in Fig. 5, where the GFP fluorescence lifetime distributions from the FLIM images are shown to shift to shorter lifetimes as the glycerol fraction increases. This is in agreement with Eq. (1), which predicts that an increasing refractive index increases the radiative rate constant  $k_r$ , which consequently shortens the fluorescence lifetime  $\tau$ . The average fluorescence lifetime of GFP-tagged proteins in cells in PBS buffer is found to be 2.4 ns, in good agreement with previous work by Treanor et al. using the same type of cells.<sup>42</sup>

Plots of the inverse lifetime as a function of the square of the refractive index show a linear relationship [Figs. 6(a) and 6(b)] similar to previous work on GFP in solution.<sup>14,15</sup> It is apparent that the fixing method does not affect the overall lifetime: The gradients of straight-line fits to the data are identical within experimental error ( $0.19 \pm 0.03 \text{ ns}^{-1}$  for BD cytofix/cytoperm and  $0.15 \pm 0.04 \text{ ns}^{-1}$  for paraformaldehyde). Furthermore, the average GFP fluorescence lifetime appears to be independent of whether the GFP is located inside or outside the plasma membrane. From the theory outlined in Sec. 1.1 and investigated in more detail

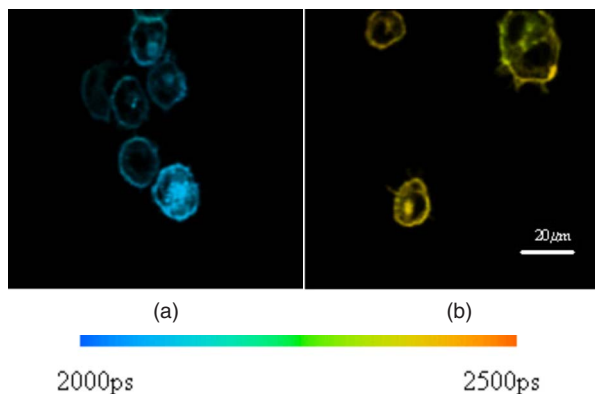


**Fig. 3** (a) FLIM image of cells expressing GFP-tagged MHC proteins in 100% glycerol solution ( $n=1.47$ ). (b) FLIM image of GFP-tagged MHC proteins in cells in PBS buffer ( $n=1.33$ ).

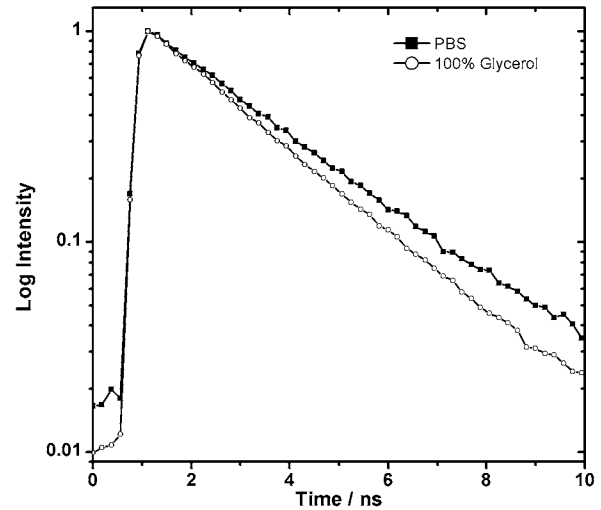


**Fig. 4** Typical decays extracted from the FLIM images of GFP-tagged cells in PBS and 100% glycerol, showing a faster fluorescence decay in the high refractive index medium.

elsewhere,<sup>37,38</sup> it is expected that the refractive index can be sensed by the fluorescence lifetime over a distance of approximately  $1 \mu\text{m}$ , i.e., over a much larger range than just the immediate local environment of a few nanometers. This is also supported by time-resolved studies of GFP in reverse micelles by Uskova et al. that appear to show that even as the reverse micelles increase in size, the refractive index of the surrounding medium can still be sensed inside via the GFP fluorescence lifetime.<sup>30</sup>

If a comparison is made between the average fluorescence lifetimes of GFP-tagged proteins in cells presented earlier and the average fluorescence lifetimes of GFP in solution,<sup>14,15</sup> a clear difference is seen in the linear relationship of inverse lifetime as a function of the square of the refractive index. The gradient of the line for GFP in cells is much shallower

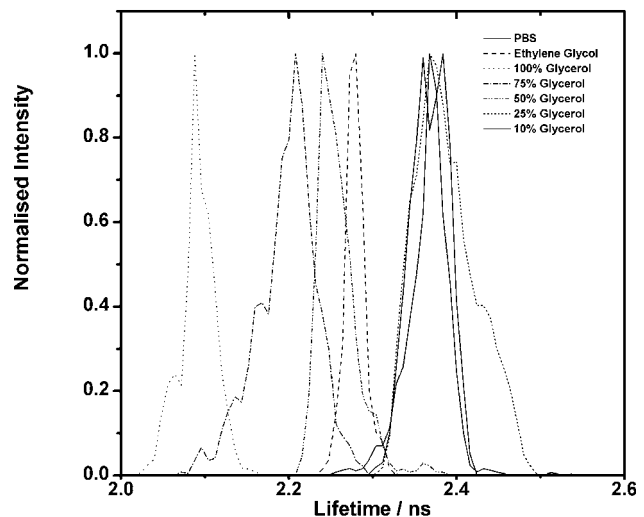


**Fig. 5** Fluorescence lifetime distributions extracted from the FLIM images of cells expressing GFP-tagged MHC protein. A clear shift to shorter lifetimes is seen as the glycerol fraction increases.

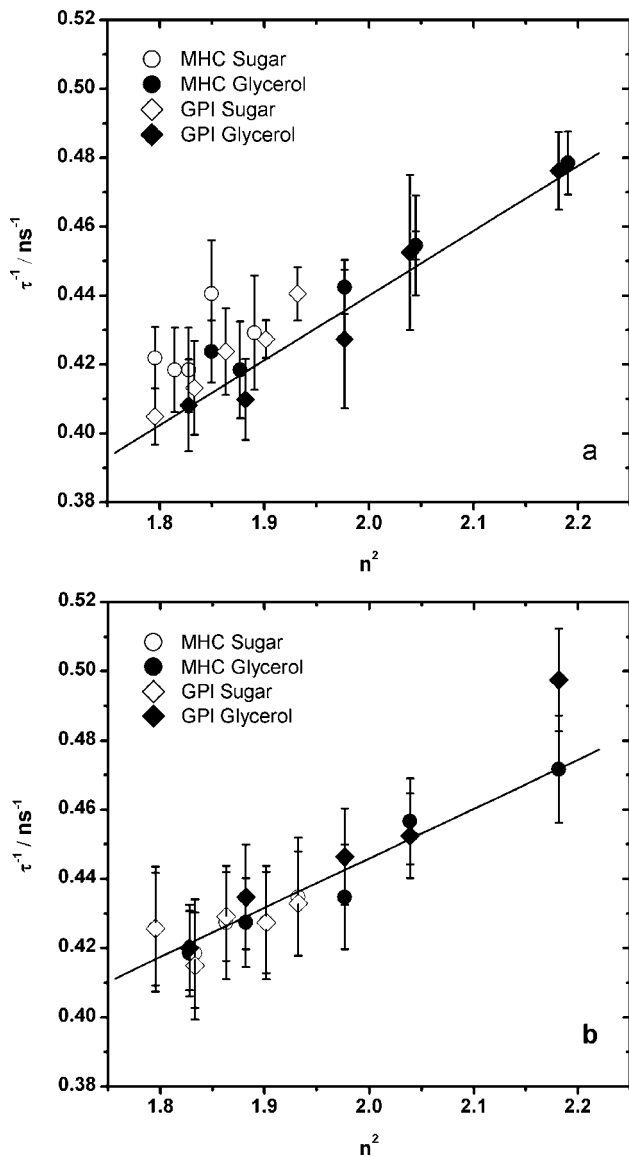


**Fig. 6** (a) Inverse average fluorescence lifetime of GFP as a function of the refractive index squared. It is evident that there is a linear correlation. This is shown for cells fixed with BD cytofix/cytoperm. (b) Inverse average fluorescence lifetime of GFP in cells fixed with 4% paraformaldehyde as a function of the refractive index squared. The gradients obtained for both fixing methods are the same within experimental error ( $0.19 \pm 0.03 \text{ ns}^{-1}$  for BD cytofix/cytoperm and  $0.15 \pm 0.04 \text{ ns}^{-1}$  for paraformaldehyde).

than that of GFP in solution [see Fig. 7(a)]. One reason for this may be because of the actual refractive index of the cells themselves. Hess et al. found that the average GFP fluorescence lifetime was shorter in cells than in buffer solution,<sup>31</sup> consistent with the idea that the cells have a higher refractive index than the buffer. Studies have been done looking at the refractive index variation across cells.<sup>46–49</sup> Beuthan et al. and Schmitt et al. find that areas in the membrane have a high refractive index due to the high concentration of lipids, making the membrane refractive index approximately 1.45.<sup>46,47,50</sup> The difference between solution and cells can therefore be

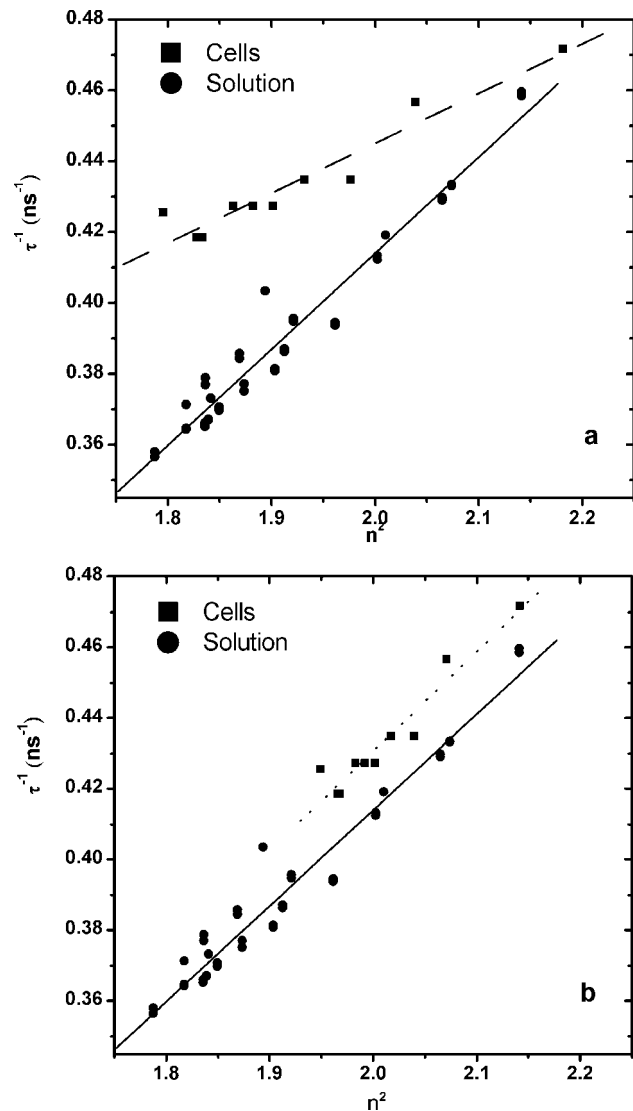


**Fig. 7** (a) Comparison of the linear relationship, before refractive index correction, between inverse average fluorescence lifetime and refractive index squared for both GFP in cells and in solution. (b) Comparison of the relationship after refractive index correction using  $n=1.45$  for the refractive index of the cell.

corrected for by calculating the average total refractive index of the system:<sup>51</sup>

$$n_{total}^2 = \frac{n_{cell}^2 + n_{sol}^2}{2}, \quad (9)$$

where  $n_{total}$  is the total refractive index of the system,  $n_{cell}$  is the refractive index of the cell ( $n=1.45$ ), and  $n_{sol}$  is the measured refractive index of the solution on the refractometer. The average is found by taking the square of the refractive index because the electric field is dependent on  $n^2$ .<sup>52</sup> By calculating  $n_{total}$ , Fig. 7(a) can be replotted using the total refractive index in place of the measured solution refractive index, and this corrects for the gradient difference [see Fig. 7(b)]. The difference in intercept could be due to the fact that the cells were measured on a different instrument or more likely is due to the complex refractive index profile of the cell as a

**Table 1** Average fluorescence lifetimes of GFP in solution at different penetration depths of the evanescent wave. As the penetration depth decreases, the average fluorescence lifetime decreases, as only molecules very close to the glass prism are excited. The GFP fluorescence lifetimes are the average of several measurements, and the error is one standard deviation.

Angle (deg)	Penetration depth ( $\mu\text{m}$ )	Lifetime (ns)
40	Bulk ( $>1$ )	$2.29 \pm 0.01$
65	0.13	$2.15 \pm 0.01$
70	0.11	$2.18 \pm 0.01$
80	0.10	$2.17 \pm 0.01$

whole.<sup>53</sup> In addition, a refined model could take account of a different weighting of  $n_{sol}$  and  $n_{cell}$ , rather than the 50:50 ratio used in Eq. (9).

The large sensing distance seen in this work does not appear to have much use for detecting changes in the local vicinity of the GFP on the nanometer scale, such as a technique like FRET. However, it has recently been claimed that the refractive index of cancer cells is apparently higher than in healthy cells.<sup>48,49</sup> Detecting fluorescence lifetime changes could therefore be useful in distinguishing healthy cells from cancerous ones. One specific area where the fluorescence lifetime dependence on the refractive index could have implications is TIRF, where a change in refractive index is key to the technique.

### 3.2 TIRF Lifetime Measurements

FLIM coupled with TIRF shows a shortening of the average fluorescence lifetime of GFP in solution at high incident angles. The evanescent wave excites only molecules in very close proximity to the glass prism, and the variation of evanescent wave penetration with varying angle is shown in Fig. 1 according to Eq. (8). Therefore, as the angle increases and the penetration depth decreases, a shortening of the fluorescence lifetime is observed. This is shown in Table 1, which shows average fluorescence lifetimes from single-point measurements of GFP in solution at different penetration depths of the evanescent wave. The average fluorescence lifetime of GFP in bulk agrees well with the value quoted in Ref. 30.

Figure 8 shows the average fluorescence lifetimes of GFP (as in Table 1) in comparison with theory from Eq. (6). These initial values show that, in a TIRF geometry, the average GFP fluorescence lifetime is shorter in comparison to the fluorescence lifetime from the bulk solution, and this is in agreement with what is expected from theory.

With the growing use of techniques such as TIRF-FRET where energy transfer is also taking place, these findings will prove very important. Changes in the average GFP fluorescence lifetime due to FRET could be hard to distinguish from changes due to the presence of the glass prism. Although there is probably little biological significance for this phenomenon, the photophysical aspect will have implications from an experimental and instrumental point of view: Care must be taken to reduce ambiguity with regard to the origin of the fluorescence lifetime change when doing time-resolved mea-

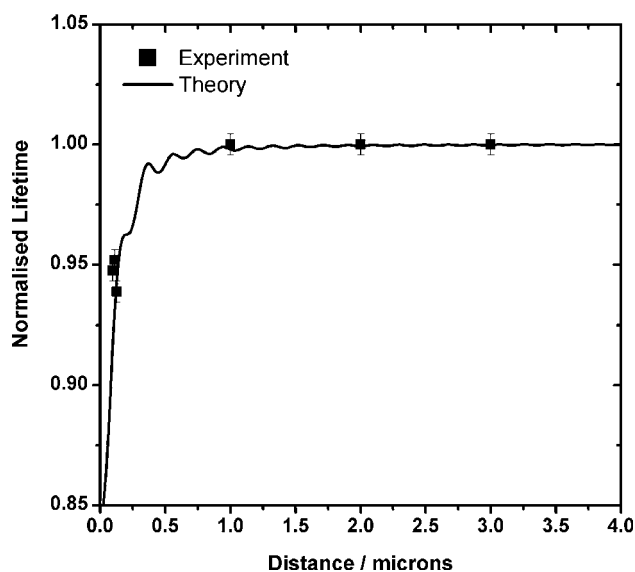


**Fig. 8** The average fluorescence lifetime of GFP as a function of distance from the glass prism interface. It is evident that as the angle increases and the penetration depth of the evanescent wave decreases, the average fluorescence lifetime of GFP also decreases, as only molecules close to the glass prism are excited. This agrees very well with what is expected from theory.

surements using TIRF microscopy. We would like to note here that this is a fundamental effect that is of course also present in intensity-based TIRF measurements, as the integrated fluorescence decay is proportional to the fluorescence intensity. The effect may be of interest for refractive index imaging,<sup>53</sup> as it allows the separation of path length and refractive index.<sup>54</sup> Last, it may be interesting to see whether the distance of a GFP-tagged protein in a cell from a glass surface could be mapped using the GFP fluorescence lifetime change.

## 4 Conclusions

This study has shown that the inverse average fluorescence lifetime of GFP-tagged proteins in cells is a function of the square of the refractive index of the medium in which the cells are suspended. When extended to investigate TIRF-FLIM, the average fluorescence lifetime of GFP in solution was found to be shorter with TIRF than with confocal microscopy due to the presence of the high refractive index prism used to produce the evanescent wave. This shortening of the fluorescence lifetime with TIRF compared to confocal microscopy could have implications when doing experiments such as TIRF-FRET where fluorescence lifetime changes are observed due to energy transfer. Therefore, care should be taken to reduce uncertainty into the cause of the fluorescence lifetime change when using TIRF microscopy.

*Note added in proof.* Since acceptance of this manuscript, refractive index sensing using GFP in living cells has been reported.<sup>55</sup>

### Acknowledgments

We would like to thank Dr. James Hunt from the Randall Division of Cell and Molecular Biophysics at King's College, London, for the kind gift of GFP. We would also like to thank

Prof. Daniel Davis from Biological Sciences at Imperial College, London, Nicolas Sergent, and Prof. David Richards from the Department of Physics at King's College, London, for stimulating and rewarding discussions.

## References

- M. Chalfie, Y. Tu, G. Euskirchen, W. W. Ward, and D. C. Prasher, "Green fluorescent protein as a marker for gene-expression," *Science* **263**(5148), 802–805 (1994).
- "Green Fluorescent Protein," in *Methods in Enzymology*, M. Conn, Ed., vol. **302**, Academic Press, San Diego (1999).
- W. B. Amos and J. G. White, "How the confocal laser scanning microscope entered biological research," *Biol. Cell* **95**(6), 335–342 (2003).
- F. S. Wouters, "The physics and biology of fluorescence microscopy in the life sciences," *Contemp. Phys.* **47**(5), 239–255 (2006).
- F. Festy, S. M. Ameer-Beg, T. Ng, and K. Suhling, "Imaging proteins *in vivo* using fluorescence lifetime microscopy," *Mol. Biosys.* **3**(6), 381–391 (2007).
- K. Suhling, "Fluorescence lifetime imaging," in *Methods Express: Cell Imaging*, D. Stephens, Ed. pp. 219–245, Scion Publishing Ltd., Bloxham (2006).
- K. Suhling, P. M. W. French, and D. Phillips, "Time-resolved fluorescence microscopy," *Photochem. Photobiol. Sci.* **4**(1), 13–22 (2005).
- M. Peter and S. M. Ameer-Beg, "Imaging molecular interactions by multiphoton FLIM," *Biol. Cell* **96**(3), 231–236 (2004).
- M. Peter, S. M. Ameer-Beg, M. K. Y. Hughes, M. D. Keppler, S. Prag, M. Marsh, B. Vojnovic, and T. Ng, "Multiphoton-FLIM quantification of the EGFP-mRFP1 FRET pair for localization of membrane receptor-kinase interactions," *Biophys. J.* **88**(2), 1224–1237 (2005).
- H. Wallrabe and A. Periasamy, "Imaging protein molecules using FRET and FLIM microscopy," *Curr. Opin. Biotechnol.* **16**(1), 19–27 (2005).
- B. Treanor, P. M. P. Lanigan, S. Kumar, C. Dunsby, I. Munro, E. Aukorsius, F. J. Culley, M. A. Purbhoo, D. Phillips, M. A. A. Neil, D. N. Burshtyn, P. M. W. French, and D. M. Davis, "Microclusters of inhibitory killer immunoglobulin like receptor signaling at natural killer cell immunological synapses," *J. Cell Biol.* **174**(1), 153–161 (2006).
- S. Pelet, M. J. R. Preville, and P. T. C. So, "Comparing the quantification of Forster resonance energy transfer measurement accuracies based on intensity, spectral, and lifetime imaging," *J. Biomed. Opt.* **11**(3), 034017-1–034017-11 (2006).
- C. Thaler, S. V. Koushik, P. S. Blank, and S. S. Vogel, "Quantitative multiphoton spectral imaging and its use for measuring resonance energy transfer," *Biophys. J.* **89**(4), 2736–2749 (2005).
- K. Suhling, D. M. Davis, Z. Petrášek, J. Siegel, and D. Phillips, "The influence of the refractive index on EGFP fluorescence lifetimes in mixtures of water and glycerol," *Proc. SPIE* **4259**, 92–101 (2001).
- K. Suhling, J. Siegel, D. Phillips, P. M. W. French, S. Lévêque-Fort, S. E. D. Webb, and D. M. Davis, "Imaging the environment of green fluorescent protein," *Biophys. J.* **83**(6), 3589–3595 (2002).
- S. F. Wuister, C. D. Donega, and A. Meijerink, "Local-field effects on the spontaneous emission rate of CdTe and CdSe quantum dots in dielectric media," *J. Chem. Phys.* **121**(9), 4310–4315 (2004).
- R. A. Lampert, S. R. Meech, J. Metcalfe, D. Phillips, and A. P. Schaap, "The refractive index correction to the radiative rate constant in fluorescence lifetime measurements," *Chem. Phys. Lett.* **94**(2), 137–140 (1983).
- S. Hirayama and D. Phillips, "Correction for Refractive Index in the Comparison of Radiative Lifetimes in Vapor and Solution Phases," *J. Photochem.* **12**(2), 139–145 (1980).
- G. Lamouche, P. Lavallard, and T. Gacoin, "Optical properties of dye molecules as a function of the surrounding dielectric medium," *Phys. Rev. A* **59**(6), 4668–4674 (1999).
- P. Lavallard, M. Rosenbauer, and T. Gacoin, "Influence of surrounding dielectrics on the spontaneous emission of sulforhodamine B molecules," *Phys. Rev. A* **54**(6), 5450–5453 (1996).
- G. Lamouche, P. Lavallard, and T. Gacoin, "Spontaneous emission of dye molecules as a function of the surrounding dielectric medium," *J. Lumin.* **76–77**, 662–665 (1998).
- D. Toptygin and L. Brand, "Fluorescence decay of DPH in lipid membranes—influence of the external refractive index," *Biophys. Chem.* **48**(2), 205–220 (1993).
- D. Toptygin, R. S. Savtchenko, N. D. Meadow, S. Roseman, and L. Brand, "Effect of the solvent refractive index on the excited-state lifetime of a single tryptophan residue in a protein," *J. Phys. Chem.* **106**(14), 3724–3734 (2002).
- J. Olmsted, "Effect of refractive index on molecular radiative lifetimes," *Chem. Phys. Lett.* **38**(2), 287–292 (1976).
- D. Magde, G. E. Rojas, and P. G. Seybold, "Solvent dependence of the fluorescence lifetimes of xanthene dyes," *Photochem. Photobiol.* **70**(5), 737–744 (1999).
- J. Mohanty and W. M. Nau, "Refractive index effects on the oscillator strength and radiative decay rate of 2,3-diazabicyclo[2.2.2]oct-2-ene," *Photochem. Photobiol. Sci.* **3**(11–12), 1026–1031 (2004).
- M. M. G. Krishna and N. Periasamy, "Fluorescence of organic dyes in lipid membranes: site of solubilization and effects of viscosity and refractive index on lifetimes," *J. Fluoresc.* **8**(1), 81–91 (1998).
- E. P. Gibson and A. J. Rest, "The determination of the refractive indexes of frozen gas matrices at 12 K by emission-spectroscopy," *Chem. Phys. Lett.* **73**(2), 294–296 (1980).
- J. W. Borst, M. A. Hink, A. van Hoek, and A. Visser, "Effects of refractive index and viscosity on fluorescence and anisotropy decays of enhanced cyan and yellow fluorescent proteins," *J. Fluoresc.* **15**(2), 153–160 (2005).
- M. A. Uskova, J. W. Borst, M. A. Hink, A. van Hoek, A. Schots, N. L. Klyachko, and A. Visser, "Fluorescence dynamics of green fluorescent protein in AOT reversed micelles," *Biophys. Chem.* **87**(1), 73–84 (2000).
- S. T. Hess, E. D. Sheets, A. Wagenknecht-Wiesner, and A. A. Heikal, "Quantitative analysis of the fluorescence properties of intrinsically fluorescent proteins in living cells," *Biophys. J.* **85**(4), 2566–2580 (2003).
- M. A. Hink, R. A. Griep, J. W. Borst, A. van Hoek, M. H. M. Eppink, A. Schots, and A. Visser, "Structural dynamics of green fluorescent protein alone and fused with a single chain Fv protein," *J. Biol. Chem.* **275**(23), 17556–17560 (2000).
- M. L. Gee, L. Lensun, T. A. Smith, and C. A. Scholes, "Time-resolved evanescent wave-induced fluorescence anisotropy for the determination of molecular conformational changes of proteins at an interface," *Euro. Biophys. J. Biophys. Lett.* **33**(2), 130–139 (2004).
- D. Axelrod, "Total internal reflection fluorescence microscopy," in *Methods in Cell Biology*, D. L. Taylor, Ed., Vol. **30**, Academic Press, Inc. pp. 246–270 (1991).
- D. Toptygin, "Effects of the solvent refractive index and its dispersion on the radiative decay rate and extinction coefficient of a fluorescent solute," *J. Fluoresc.* **13**(3), 201–219 (2003).
- S. J. Strickler and R. A. Berg, "Relationship between absorption intensity and fluorescence lifetime of molecules," *J. Chem. Phys.* **37**(4), 814–822 (1962).
- C. Jones and K. Suhling, "Mapping the refractive index sensing range of the GFP fluorescence decay with FLIM," *Proc. SPIE* **6098**, 609807-1–609807-11 (2006).
- C. Jones and K. Suhling, *J. Phys.: Conf. Ser.* **45**, 266–273 (2006).
- H. Kuhn, "Classical aspects of energy transfer in molecular systems," *J. Chem. Phys.* **53**(1), 101–108 (1970).
- K. H. Tews, "On the variation of luminescence lifetime. The approximations of the approximative methods," *J. Lumin.* **9**, 223–239 (1974).
- K. Drexhage, "Influence of a dielectric interface on fluorescence decay time," *J. Lumin.* **1,2**, 693–701 (1970).
- B. Treanor, P. M. P. Lanigan, K. Suhling, T. Schreiber, I. Munro, M. A. A. Neil, D. Phillips, D. M. Davis, and P. M. W. French, "Imaging fluorescence lifetime heterogeneity applied to GFP-tagged MHC protein at an immunological synapse," *J. Microsc.* **217**, 36–43 (2005).
- D. M. Davis, I. Chiu, M. Fassett, G. B. Cohen, O. Mandelboim, and J. L. Strominger, "The human natural killer cell immune synapse," *Proc. Natl. Acad. Sci. U.S.A.* **96**(26), 15062–15067 (1999).
- L. M. Carlin, K. Eleme, F. E. McCann, and D. M. Davis, "Intercellular transfer and supramolecular organization of human leukocyte antigen C at inhibitory natural killer cell immune synapses," *J. Exp. Med.* **194**(10), 1507–1517 (2001).
- B. Onfelt, S. Nedvetzki, K. Yanagi, and D. M. Davis, "Cutting edge: membrane nanotubes connect immune cells," *J. Immunol.* **173**(3), 1511–1513 (2004).
- J. Beuthan, O. Minet, J. Helfmann, M. Herrig, and G. Müller, "The spatial variation of the refractive index in biological cells," *Phys.*

- Med. Biol.* **41**(3), 369–382 (1996).
47. J. M. Schmitt and G. Kumar, “Turbulent nature of refractive index variations in biological tissue,” *Opt. Lett.* **21**(16), 1310–1312 (1996).
  48. W. Z. Song, X. M. Zhang, A. Q. Liu, C. S. Lim, P. H. Yap, and H. M. M. Hosseini, “Refractive index measurement of single living cells using on-chip Fabry-Perot cavity,” *Appl. Phys. Lett.* **89**(20), 203901 (2006).
  49. X. J. Liang, A. Q. Liu, C. S. Lim, T. C. Ayi, and P. H. Yap, “Determining refractive index of single living cell using an integrated microchip,” *Sens. Actuators, A* **133**(2), 349–354 (2007).
  50. S. Johnsen and E. A. Widder, “The physical basis of transparency in biological tissue: ultrastructure and the minimization of light scattering,” *J. Theor. Biol.* **199**(2), 181–198 (1999).
  51. A. Petukhova, A. S. Paton, I. Gourevich, E. Kumacheva, J. J. Saarinen, and J. E. Sipe, “Extinction analysis of dielectric multilayer microspheres,” *Appl. Phys. Lett.* **89**(21), 211908 (2006).
  52. E. Hecht, *Optics*, 4th ed., Addison Wesley, Reading, MA (2002).
  53. W. Choi, C. Fang-Yen, K. Badizadegan, S. Oh, N. Lue, R. R. Dasari, and M. S. Feld, “Tomographic phase microscopy,” *Nat. Methods* **4**(9), 717–719 (2007).
  54. C. L. Curl, C. J. Bellair, T. Harris, B. E. Allman, P. J. Harris, A. G. Stewart, A. Roberts, K. A. Nugent, and L. M. D. I. Delbridge, “Refractive index measurement in viable cells using quantitative phase-amplitude microscopy and confocal microscopy,” *Cytometry* **65A**, 88–92 (2005).
  55. H.-J. van Manen, P. Verkuijlen, P. Wittendorp, V. Subramaniam, T. K. van den Berg, D. Roos, and C. Otto, “Refractive index sensing of green fluorescent proteins in living cells using fluorescence lifetime imaging microscopy,” *Biophys. J.* **94**(8), L67–L69 (2008).